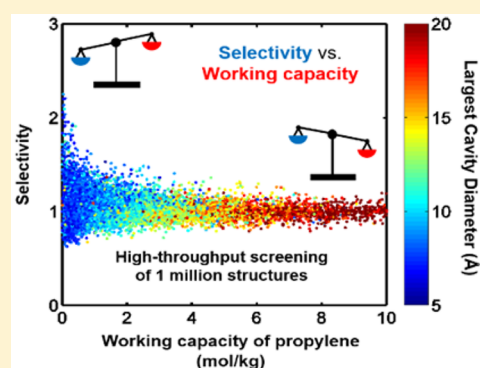


High-Throughput Screening to Investigate the Relationship between the Selectivity and Working Capacity of Porous Materials for Propylene/Propane Adsorptive Separation

Byung Chul Yeo,^{†,‡} Donghun Kim,[†] Hyungjun Kim,[‡] and Sang Soo Han^{*,†}[†]Computational Science Research Center, Korea Institute of Science and Technology (KIST), Hwarangno 14-gil 5, Seoul 02792, Republic of Korea[‡]School of Electrical and Electronic Engineering, Yonsei University, Seoul 03722, Republic of Korea

S Supporting Information

ABSTRACT: An efficient propylene/propane separation is a very critical process for saving the cost of energy in the petrochemical industry. For separation based on the pressure-swing adsorption process, we have screened ~1 million crystal structures in the Cambridge Structural Database and Inorganic Crystal Structural Database with descriptors such as the surface area of N₂, accessible surface area of propane, and pore-limiting diameter. Next, grand canonical Monte Carlo simulations have been performed to investigate the selectivities and working capacities of propylene/propane under experimental process conditions. Our simulations reveal that the selectivity and the working capacity have a trade-off relationship. To increase the working capacity of propylene, porous materials with high largest cavity diameters (LCDs) and low propylene binding energies (Q_{st}) should be considered; conversely, for a high selectivity, porous materials with low LCDs and high propylene Q_{st} should be considered, which leads to a trade-off between the selectivity and the working capacity. In addition, for the design of novel porous materials with a high selectivity, we propose a porous material that includes elements with a high crossover distance in their Lennard-Jones potentials for propylene/propane such as In, Te, Al, and I, along with the low LCD stipulation.



1. INTRODUCTION

Olefin/paraffin separation in the petrochemical industry is a very important and energy-intensive process, and thus, an improvement in the process efficiency can lead to a reduction of the manufacturing cost and to a design of more eco-friendly manufacturing systems.¹ Among various olefins, propylene (C₃H₆) is an essential component in various household plastic products, and it is obtained by separating propylene (C₃H₆)/propane (C₃H₈) mixtures produced during the petroleum refining process. Propylene/propane separation is a difficult process because the two molecules have similar sizes and chemical properties. Accordingly, the development of relevant separation technologies is very valuable.

For over 80 years, cryogenic distillation has been used for the separation; however, it is the most energy-intensive distillation.² As promising alternatives, there are physical adsorption processes such as pressure-swing adsorption (PSA) or membrane separation. Membrane separation is more energy-efficient than PSA; however, the purity of gases obtained by PSA is significantly better.³ Therefore, in this work, we consider the PSA process.

For the PSA process, porous materials with selective adsorption properties are required,⁴ and various porous materials such as zeolites, metal organic frameworks (MOFs),

and zeolitic imidazolate frameworks (ZIFs) have been reported so far. Among these, zeolites have already been used for separation, purification, and catalysis in the petroleum refining industry.^{5,6} On the other hand, the development of MOFs or ZIFs with nanoporous crystalline structures has generated explosive interest in the field of gas adsorption/separation^{7–22} because they usually have higher surface area or porosity than zeolites. In addition, the MOF and ZIF structures are comprised of metallic nodes and organic linkers, through which their shape, porosity, and functionality can be tuned by changing the types of the metallic nodes and organic linkers; this tuning ability has resulted in an exponential increase in the number of synthesized MOFs/ZIFs.^{23,24}

Recently, high-throughput computational screening has been regarded as an efficient method of designing novel functional materials, and it has been pursued in various material science fields such as lithium ion batteries,^{25,26} catalysts,^{27,28} and more.²⁹ The high-throughput approach has also been taken for gas storage and separation using porous materials.³⁰ In particular, previous works on gas storage using the high-

Received: August 12, 2016

Revised: October 5, 2016

Published: October 5, 2016

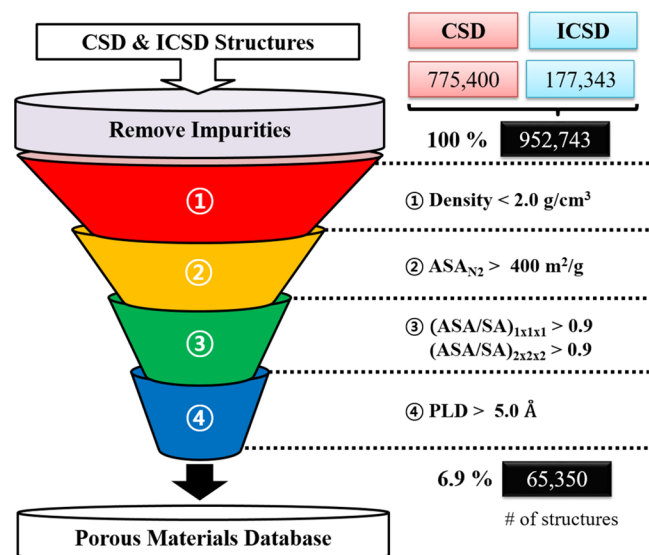
throughput approach have paid attention to H₂³¹ and CH₄ storage^{32–34} and CO₂ capture.³⁵ For gas separation, the separation of ethane/ethylene,³⁶ *p*-xylene,³⁷ CO₂,^{38,39} and noble gases (e.g., Xe/Kr)^{40,41} has been investigated. To the best of our knowledge, there has been no high-throughput screening study on the separation of propylene/propane, which is the focus of this work.

In this work, for propane/propylene separation, we screened approximately one million (1 000 000) structures in the Cambridge Structural Database (CSD)⁴² and Inorganic Crystal Structural Database (ICSD)⁴³ and performed grand canonical Monte Carlo (GCMC) simulations. Then, we analyzed correlations between the working capacity, selectivity, and physical properties (e.g., the heat of adsorption, surface area, pore volume, and largest cavity diameter) of porous materials. We find that both the working capacity and the selectivity are significantly affected by the cavity diameters and the types of elements near cavities, and the two properties have a trade-off relationship.

2. COMPUTATIONAL DETAILS

Development of a Structure Database of Porous Materials. In this work, we explore the working capacity and the selectivity of porous materials as key properties for the PSA separation of propylene/propane, where the properties are obtained from GCMC simulations for adsorption isotherms of pure gases. Prior to the GCMC simulations for a huge number of porous materials, a structural database for the materials is required. A flow diagram showing a high-throughput screening procedure to obtain a database of porous materials from all structures in the CSD and ICSD is summarized in Scheme 1.

Scheme 1. Flow Diagram Showing a High-Throughput Screening Procedure to Obtain a Database of Porous Materials from All Structures in the CSD and ICSD



We downloaded all crystal structures in the CSD and ICSD, including 775 400 and 177 343 structures, respectively. Here, because each crystal structure entry in both the CSD and ICSD might have impurities that are solvent molecules, which mainly include carbon, oxygen, and hydrogen atoms, such impurities must be removed to obtain full porosity of the materials. We automatically removed the impurities with information

regarding their bond connectivities and coordination numbers. The bond connectivity is determined by the distances between atom pairs. When the distance between atom pairs is shorter than the distance calculated on the basis of the covalent radii of both atoms, the atom pair is considered to have a bond connection. If guest atoms or molecules have no bond connectivity with adsorbent atoms, they are removed. However, in spite of the application of this method, all of the impurities are not perfectly removed in several MOF/ZIF cases. Thus, we also considered the coordination number. MOFs and ZIFs consist of two components: metallic nodes and organic linkers, where each organic linker is connected to more than two metallic nodes. If the coordination number of the guest atoms or molecules is one, we regard the guest atoms or molecules as impurities and remove them. An example of the removal process of the impurities is shown in Figure S1.

The CSD and ICSD include not only porous materials but also various condensed materials such as metals, semiconductors, and metal oxides. Therefore, prior to GCMC simulation, it is necessary to extract only porous materials from the databases. To do this, we filtered the CSD and ICSD using several screening descriptors such as density, surface area (SA), and pore limit diameter (PLD), where the SA and PLD were calculated with the open-source Zeo++ software package.⁴⁴

As a reference value for the density for the screening procedure, we used 2.0 g/cm³ because the densities of zeolites, MOFs, and ZIFs are typically less than this value. For example, most zeolites have densities of <2.0 g/cm³,⁴⁵ MOFs have densities of <1.0 g/cm³,⁴⁶ and ZIFs have densities of <1.5 g/cm³.^{47,48}

The SA is one of the representative properties in evaluating the porosity of materials. The BET (Brunauer–Emmett–Teller) method using N₂ gas is commonly used to experimentally measure the SAs of materials. On the other hand, three methods, such as van der Waals surface, Connolly surface, and accessible surface, are usually considered for the theoretical determination of the SA, where each definition can be found in ref 49. Among these, it was reported that the accessible surface area (ASA) matches well with the experimental BET surface area.⁵⁰ Thus, we calculated the solvent ASA of the crystal structures with the Zeo++ program, where a probe radius (1.86 Å) corresponding to N₂ was considered. We used a reference value of 400 m²/g for the ASA screening procedure because most MOFs and ZIFs have higher SAs than 400 m²/g,^{46–48} although there are several zeolites with SAs < 400 m²/g.

Porous materials in the CSD and ICSD may have isolated pores to which propane and propylene gases are experimentally inaccessible. However, GCMC simulations might predict that the propylene and propane molecules exist in a pore if the pore is bigger than the size of the molecules, which leads to a discrepancy between experimental and simulation results. Thus, we excluded crystal structures with such isolated pores to formulate GCMC simulations. For the simulations, we also considered the ASA/SA screening descriptor, where both the ASA and the SA were calculated with a probe diameter of 5.0 Å, which corresponds to propane because the propane size is bigger than the propylene size (4.68 Å).⁵¹ When the ASA/SA ratio is 1, the material has no isolated pores (a propane molecule is accessible to all pores). For the screening procedure with the ASA/SA, we used 0.9 as a reference value, which allows for a small error margin. After the screening procedure, we discovered several crystal structures with isolated pores

although the ASA/SA ratio calculated with the unit cell of the crystals had been satisfied with the screening condition ($ASA/SA > 0.9$). Thus, we double-checked the ASA/SA for the $2 \times 2 \times 2$ supercell structures. A relevant example of this can be found in Figure S2.

For the PSA separation of propylene and propane, the porous materials should have pores or cavities into which propane and propylene molecules can penetrate. To satisfy this requirement, we also considered the PLD of porous materials, which represents the diameter of the circular gate of the maximum cavity in a porous material (Figure S3). The entrance size in the porous structure should be larger than the molecular size of propane (5.0 Å), which is larger than that of propylene. Thus, we set the requirement that the PLD is larger than 5.0 Å.

Calculation of Propane and Propylene Uptake Amount. After all of the screening processes, the numbers of the porous materials obtained from the CSD and ICSD are 64 182 and 1168, respectively, which gives a total number of 65 350 (6.9%). For these structures, we simulated equilibrium adsorption isotherms for both propane and propylene by GCMC simulations from 0 to 500 kPa at 400 K, which are within the range of the operating conditions for a practical PSA separation process.⁵² To obtain an accurate measure of propane and propylene loading, we considered 10^7 configurations to compute the average loading for each condition. The GCMC simulations were performed by the open source MUSIC software⁵³ employed with periodic boundary conditions along all x , y , and z directions.

For the GCMC simulation, force fields (FFs) are required between adsorbent and adsorbate as well as between adsorbates. In this work, the interaction energies were computed through the Lennard-Jones (LJ) potential, where the parameters for the adsorbent atoms were taken from the Universal Force Field (UFF)⁵⁴ and those for the adsorbate (propylene and propane) components (e.g., CH_3 , CH_2 , and CH) were taken from the standard TraPPE-UA force fields.⁵⁵ The FFs for the CH_3 , CH_2 , and CH components in propane and propylene molecules are summarized in Table S1. In addition, the LJ parameters between adsorbent atoms and the components of the adsorbate were calculated using the Lorentz–Berthelot mixing rules.⁵⁶ To validate the FFs, we simulated the densities of propane and propylene in the gas phase at 400 K and compared the results with experimental values.⁵⁷ As shown in Figure S4, our simulation matches well the experimental densities. In addition, our simulation reproduces the experimental adsorption isotherm for propylene and propane on zeolite 13X⁵⁸ (Figure S5) and ZIF-8⁵⁹ (Figure S6).

Several porous materials show a flexible structure property upon inclusion or removal of adsorbate gases or solvents. However, we assumed that after removing the solvents the structures are not collapsed and that during the GCMC simulation, they are rigid.

3. RESULTS AND DISCUSSION

To estimate the performance of porous materials for the PSA separation of propylene/propane, we considered a working capacity and a selectivity that were calculated from the adsorption isotherms of propane and propylene. Here, the working capacity (W) is defined as the difference between the capacities of the adsorption (500 kPa) and the desorption (50 kPa) pressures: $W = N_{500\text{kPa}} - N_{50\text{kPa}}$. The selectivity (S) is defined as the ratio of the adsorption amount of propylene over

that of propane at the adsorption pressure (500 kPa):

$$S = \frac{N_{\text{C}_3\text{H}_6, 500\text{kPa}}}{N_{\text{C}_3\text{H}_8, 500\text{kPa}}}$$

The working capacity and the selectivity were calculated on the basis of adsorption capacities at 50 and 500 kPa. Accordingly, to understand the correlation between the working capacity/selectivity and the physical properties of the porous materials, we first investigated the correlation between the adsorption capacities of propylene at 50 and 500 kPa and several physical properties of porous materials (see Figure S7). A correlation between the adsorption capacity and the physical property was quantized using Pearson's correlation coefficient (ρ_{corr}):⁶⁰

$$\rho_{\text{corr}} = \frac{E[(X - \mu_X)(Y - \mu_Y)]}{\sigma_X \sigma_Y}$$

where σ_X is the standard deviation of X , μ_X is the mean of X , and E is the expectation.

Here, we considered four physical properties: the isosteric heat of adsorption (Q_{st}), surface area, pore volume, and largest cavity diameter (LCD). Two porous materials can have similar pore volumes even though their pore structures are significantly different, as shown in Figure S8. Here, the LCD is an efficient indicator used to distinguish the pore structures of such porous materials. Thus, we considered the LCD as one of the main physical properties.

Figure 1a shows Pearson's correlation coefficients for correlations between the four physical properties and the uptake amount of propylene at 50 and 500 kPa. At 50 kPa, the propylene uptake is observed to be the most closely correlated with the Q_{st} ; however, at 500 kPa, the LCD has the highest correlation coefficient. To increase the working capacity of propylene, the uptake amount at 500 kPa should be maximized, while the amount at 50 kPa should be minimized. Therefore, a high working capacity can be observed in a porous material with a high LCD as well as a low Q_{st} , which is confirmed in Figure 1b. A similar behavior is also found in the case of propane. On the other hand, the selectivity is defined as the ratio of the uptake amounts of propylene and propane at 500 kPa, which we expect that it would be mainly affected by the LCD. Indeed, a lower LCD provides a higher selectivity, as observed in Figure 1c.

From Figure 1, the higher LCD provides a higher working capacity but a lower selectivity, which indicates that the working capacity and the selectivity have a trade-off relationship with the LCD. Figure 2 clearly shows the trade-off relationship between the selectivity and the working capacity. Here, the following intriguing questions arise: (1) Why does a lower LCD usually lead to a higher selectivity of propylene? (2) Why do porous materials with similar LCDs have selectivities with different values? (Why does the selectivity have a range of values at a given LCD value?)

To find an answer to the first question, we investigated LJ potential surfaces between adsorbent atoms and propane/propylene molecules. In Figure 3a, we representatively compare the LJ potentials between the adsorbate molecules and the carbon atom of the adsorbents. Here, a crossover point of the potential energies is observed at 3.9 Å, where at distances below the crossover point, the LJ potentials of propylene show lower energy values (more favorable adsorption) and vice versa. A similar phenomenon is observed for all atoms of the adsorbents. The LJ potential result indicates that in a small

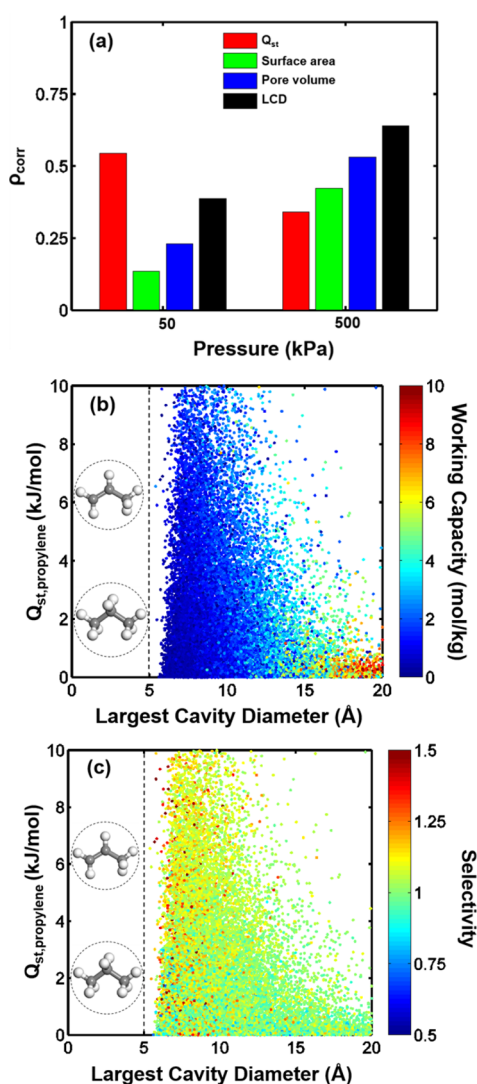


Figure 1. (a) Pearson's correlation coefficients for correlations between the four physical properties (Q_{st} , surface area, pore volume, and LCD) and uptake amounts of propylene at 50 and 500 kPa. Here, the two pressures indicate desorption and adsorption pressures for the PSA separation, respectively. (b) Two-dimensional plot for correlations between Q_{st} (propylene), LCD, and the working capacity of propylene, where the Q_{st} is calculated at 50 kPa (the desorption pressure). (c) Two-dimensional plot for correlations between Q_{st} (propylene), LCD, and selectivity, where the Q_{st} is calculated at 500 kPa (the adsorption pressure). In b and c, the propane and propylene molecules are included to compare their molecular sizes and the LCDs.

cavity, the adsorption of propylene could be more favorable than the adsorption of propane, which leads to a higher selectivity of propylene. To support this argument, we have also calculated the selectivity of propylene with bundles of (7, 7) (LCD: 6.1 Å) and (10, 10) (LCD: 10.2 Å) carbon nanotubes (CNTs) through which we can focus on the effect of LCD on the selectivity without considering the effects of different elements. Indeed, the (7, 7) CNT with a smaller LCD shows a selectivity of 1.67, which is higher than the selectivity (1.23) of (10, 10) CNT (Figure S10).

Moreover, the potential energy surface is dependent on the elements used, which implies that although they have the same LCD, porous materials containing different elements can have

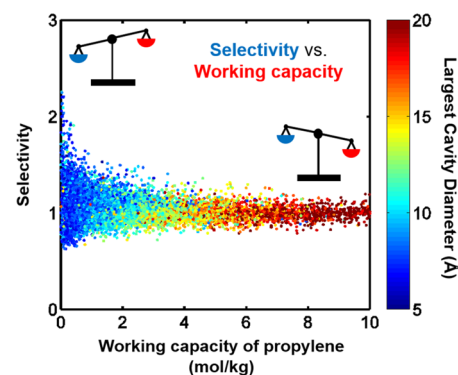


Figure 2. Two-dimensional plot for correlations between the selectivity, working capacity of propylene, and LCD.

different uptake amounts of propylene and can provide different degrees of selectivity of propylene. We have summarized the crossover distance for the various elements mentioned in Figure 3a, as shown in Figure 3c. A longer crossover distance for a given cavity leads to a more favorable region of propylene adsorption. For example, consider two nanotube structures composed of only silicon (Si) or carbon (C) atoms. According to Figure 3c, Si has a longer crossover distance than C. Thus, of the two nanotubes, the silicon nanotube (SiNT) could have a higher selectivity than CNT for a given LCD (Figure S10). From these observations, it is clear that elements in the cavities can also significantly affect the selectivity, along with the LCD. We can also expect that porous materials containing elements (e.g., In, Te, Al, and I) with a high crossover point would provide a high selectivity of propylene.

In Figure 2, it is observed that a range of the selectivity value is much wider as the LCD decreases. This can be explained with the LJ potential shown in Figure 3a. Because the repulsive energy increases more steeply than the attractive energy, the energy difference between propylene-adsorbent and propane-adsorbent is more significant as the distance between them decreases. Therefore, porous materials with lower LCDs (small cavities) show a wider range of selectivity of propylene.

Moreover, from the explanations presented thus far, the selectivity can be significantly affected by not only the LCD but also by the binding energies (Q_{st}). In Figure 3d, it is clear that the porous materials with a higher Q_{st} of propylene over the Q_{st} of propane show higher selectivities of propylene.

For the high efficiency of the propane/propylene separation process, it would be ideal to maximize both the selectivity and the working capacity. Thus, the product ($S \times W$) of the selectivity (S) and working capacity (W) can be defined as a metric that indicates the performance of a given structure.³⁶ Assuming $S \times W > 10$ as a reference for the high-performing material, 442 porous materials fall below the high-performing region. In addition, the $S \times W$ property is observed to be the most closely correlated with the LCD; however, the Q_{st} and the pore volume are also important factors to determine the property, which is supported by Figure S11.

In this work, we assumed that propylene interactions with an unsaturated (open) metal site in porous materials are the same as that with saturated metals sites, although a porous material with the open-metal site has a strong interaction with olefins via π -complexation.^{17,61–64} Thus, it is necessary to further investigate effects of open-metal sites in MOFs on the selectivity and working capacity. We compared the UFF (the

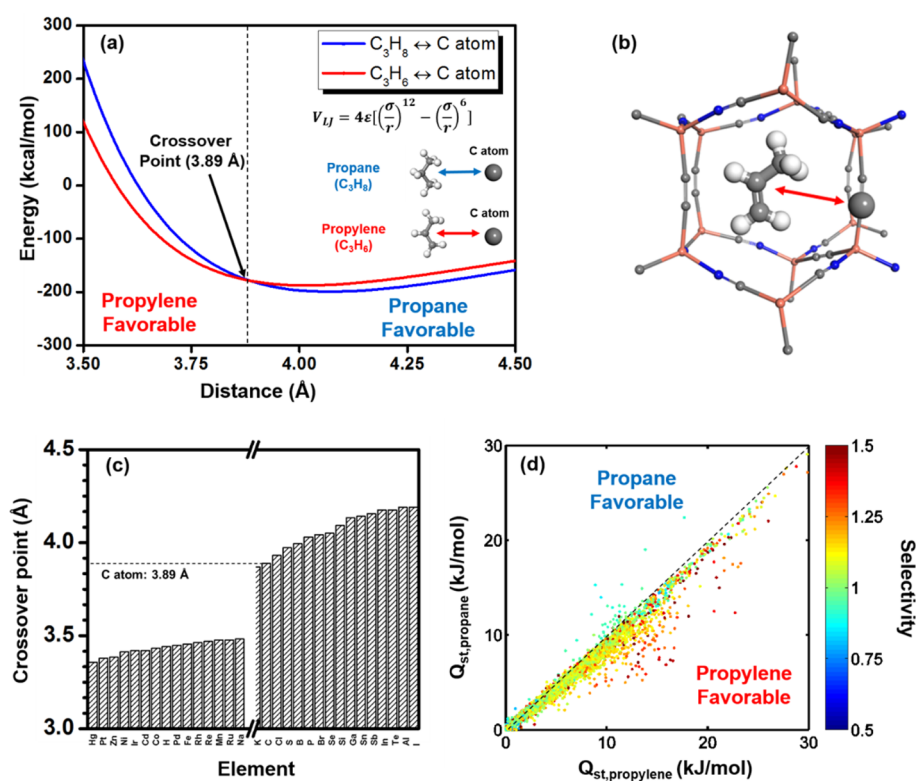


Figure 3. (a) The Lennard-Jones (LJ) potential surfaces for propane...carbon and propylene...carbon as a function of distance, where the carbon atom is assumed to be a representative of atoms consisting of porous materials (adsorbents) shown in b. (c) The crossover points for elements in a periodic table, which are calculated by the LJ potentials for propane and propylene...element, such as in a. More information can be found in Figure S9. (d) Correlation between the selectivity and Q_{st} of propylene/propane.

default FF of this work for adsorbents) and the modified FF⁶¹ considering the effect of the open-metal site by calculating equilibrium adsorption isotherms of propane and propylene in HKUST-1 in Figure S12. Indeed, the UFF underestimates the propylene uptake amount in the HKUST-1 in comparison to the experimental value, although it provides a reasonable agreement for the propane uptake. On the other hand, the modified FF reported in ref 61 leads to more accurate results for the propylene uptake in HKUST-1. However, although the effect of open-metal sites is further considered, the conclusion indicating a trade-off relationship between the selectivity and the working capacity is unchanged, as shown in Figure S13.

4. CONCLUSION

In summary, for the PSA process of propylene/propane separation, we have performed a high-throughput screening of ~1 million structures in the CSD and ICSD and GCMC simulations. Our simulations reveal a trade-off relationship between the selectivities and the working capacities that are key properties of porous materials for propylene/propane separation. To increase the working capacity of propylene, porous materials with high LCD and low propylene Q_{st} values should be considered; conversely, to achieve a high selectivity, porous materials with low LCD and high propylene Q_{st} values should be considered. Because of these reasons, the selectivity and the working capacity have a trade-off relationship. In addition, as an aspect of designing new porous materials with a high selectivity of propylene, we suggest the inclusion of elements with a high crossover point in the LJ potentials for propylene/propane, such as In, Te, Al, and I, along with the low LCD stipulation.

■ ASSOCIATED CONTENT

Supporting Information

The Supporting Information is available free of charge on the ACS Publications website at DOI: 10.1021/acs.jpcc.6b08177.

Computational details including an impurity removal process, a selection process of porous materials with isolated pores, a force field, and a validation result of our GCMC simulation. Pearson's correlation coefficients of the correlations between the propylene uptake amount and various physical properties of porous materials. The crossover point for all elements in the periodic table. The calculated selectivity of propylene for various CNTs and SiNTs.

(PDF)

■ AUTHOR INFORMATION

Corresponding Author

*E-mail: sangsoo@kist.re.kr. Tel.: +82 2 958 5441. Fax: +82 2 958 5451.

Notes

The authors declare no competing financial interest.

■ ACKNOWLEDGMENTS

This work was supported by Creative Materials Discovery Program through the National Research Foundation of Korea (NRF-2016M3D1A1021140). We acknowledge the financial supports of the Korea Institute of Science and Technology (Grant No. 2E26130).

REFERENCES

- (1) Cadiau, A.; Adil, K.; Bhatt, P. M.; Belmabkhout, Y.; Eddaoudi, M. A Metal-Organic Framework-Based Splitter for Separating Propylene from Propane. *Science* **2016**, *353*, 137–140.
- (2) U.S. Department of Energy (DOE). *Materials for Separation Technology: Energy and Emission Reduction Opportunities*, 2005.
- (3) Feng, X.; Pan, C. Y.; Ivory, J.; Ghosh, D. Integrated Membrane/adsorption Process for Gas Separation. *Chem. Eng. Sci.* **1998**, *53*, 1689–1698.
- (4) Grande, C. A.; Gascon, J.; Kapteijn, F.; Rodrigues, A. E. Propane/propylene Separation with Li-Exchanged Zeolite 13X. *Chem. Eng. J.* **2010**, *160*, 207–214.
- (5) Ackley, M. W.; Yang, R. T. Adsorption Characteristics of High-Exchange Clinoptilolites. *Ind. Eng. Chem. Res.* **1991**, *30*, 2523–2530.
- (6) Yang, R. T. *Gas Separation by Adsorption Process*; Imperial College Press: London, 1997.
- (7) Murray, L. J.; Dincă, M.; Long, J. R. Hydrogen Storage in Metal-organic Frameworks. *Chem. Soc. Rev.* **2009**, *38*, 1294–1314.
- (8) Dincă, M.; Dailly, A.; Liu, Y.; Brown, C. M.; Neumann, D. A.; Long, J. R. Hydrogen Storage in a Microporous Metal-Organic Framework with Exposed Mn²⁺ Coordination Sites. *J. Am. Chem. Soc.* **2006**, *128*, 16876–16883.
- (9) Han, S. S.; Goddard, W. A., III. Lithium-Doped Metal-Organic Frameworks for Reversible H₂ Storage at Ambient Temperature. *J. Am. Chem. Soc.* **2007**, *129*, 8422–8423.
- (10) Blomqvist, A.; Araújo, C. M.; Srepusharawoot, P.; Ahuja, R. Li-decorated Metal-Organic Framework 5: A Route to Achieving a Suitable Hydrogen Storage Medium. *Proc. Natl. Acad. Sci. U. S. A.* **2007**, *104*, 20173–20176.
- (11) Latroche, M.; Surlblé, S.; Serre, C.; Mellot-Draznieks, C.; Llewellyn, P. L.; Lee, J. H.; Chang, J. S.; Sung, H. J.; Férey, G. Hydrogen Storage in the Giant-Pore Metal-Organic Frameworks MIL-100 and MIL-101. *Angew. Chem., Int. Ed.* **2006**, *45*, 8227–8231.
- (12) Ma, S.; Zhou, H. C. Gas Storage in Porous Metal-Organic Frameworks for Clean Energy Applications. *Chem. Commun.* **2010**, *46*, 44–53.
- (13) Klontzas, E.; Mavrandonakis, A.; Tylianakis, E.; Froudakis, G. E. Improving Hydrogen Storage Capacity of MOF by Functionalization of the Organic Linker with Lithium Atoms. *Nano Lett.* **2008**, *8*, 1572–1576.
- (14) Mavrandonakis, A.; Klontzas, E.; Tylianakis, E.; Froudakis, G. E. Enhancement of Hydrogen Adsorption in Metal-Organic Frameworks by the Incorporation of the Sulfonate Group and Li Cations. A Multiscale Computational Study. *J. Am. Chem. Soc.* **2009**, *131*, 13410–13414.
- (15) Mavrandonakis, A.; Tylianakis, E.; Stubos, A. K.; Froudakis, G. E. Why Li Doping in MOFs Enhances H₂ Storage Capacity? A Multi-Scale Theoretical Study. *J. Phys. Chem. C* **2008**, *112*, 7290–7294.
- (16) Klontzas, E.; Tylianakis, E.; Froudakis, G. E. Designing 3D COFs with Enhanced Hydrogen Storage Capacity. *Nano Lett.* **2010**, *10*, 452–454.
- (17) Li, J. R.; Kuppler, R. J.; Zhou, H. C. Selective Gas Adsorption and Separation in Metal-Organic Frameworks. *Chem. Soc. Rev.* **2009**, *38*, 1477–1504.
- (18) An, J.; Geib, S. J.; Rosi, N. L. High and Selective CO₂ Uptake in a Cobalt Adeninate Metal-Organic Framework Exhibiting Pyrimidine- and Amino-Decorated Pores. *J. Am. Chem. Soc.* **2010**, *132*, 38–39.
- (19) Bae, Y. S.; Snurr, R. Q. Development and Evaluation of Porous Materials for Carbon Dioxide Separation and Capture. *Angew. Chem., Int. Ed.* **2011**, *50*, 11586–11596.
- (20) Wang, B.; Côté, A. P.; Furukawa, H.; O’Keeffe, M.; Yaghi, O. M. Colossal Cages in Zeolitic Imidazolate Frameworks as Selective Carbon Dioxide Reservoirs. *Nature* **2008**, *453*, 207–211.
- (21) Thallapally, P. K.; Tian, J.; Kishan, M. R.; Fernandez, C. A.; Dalgarno, S. J.; McGrail, P. B.; Warren, J. E.; Atwood, J. L. Flexible (Breathing) Interpenetrated Metal-Organic Frameworks for CO₂ Separation Applications. *J. Am. Chem. Soc.* **2008**, *130*, 16842–16843.
- (22) Couck, S.; Denayer, J. F. M.; Baron, G. V.; Re, T.; Gascon, J.; Kapteijn, F. An Amine-Functionalized MIL-53 Metal - Organic Framework with Large Separation Power for CO₂ and CH₄. *J. Am. Chem. Soc.* **2009**, *131*, 6326–6327.
- (23) Furukawa, H.; Cordova, K. E.; O’Keeffe, M.; Yaghi, O. M. The Chemistry and Applications of Metal-Organic Frameworks. *Science* **2013**, *341*, 1230444–1230444.
- (24) Chen, B.; Yang, Z.; Zhu, Y.; Xia, Y. Zeolitic Imidazolate Framework Materials: Recent Progress in Synthesis and Applications. *J. Mater. Chem. A* **2014**, *2*, 16811–16831.
- (25) Ceder, G. Opportunities and Challenges for First-Principles Materials Design and Applications to Li Battery Materials. *MRS Bull.* **2010**, *35*, 693–701.
- (26) Ceder, G.; Hautier, G.; Jain, A.; Ong, S. P. Recharging Lithium Battery Research with First-principles Methods. *MRS Bull.* **2011**, *36*, 185–191.
- (27) Greeley, J.; Jaramillo, T. F.; Bonde, J.; Chorkendorff, I. B.; Nørskov, J. K. Computational High-Throughput Screening of Electrocatalytic Materials for Hydrogen Evolution. *Nat. Mater.* **2006**, *5*, 909–913.
- (28) Studt, F.; Abild-Pedersen, F.; Bligaard, T.; Sørensen, R. Z.; Christensen, C. H.; Nørskov, J. K. Identification of Non-Precious Metal Alloy Catalysts for Selective Hydrogenation of Acetylene. *Science* **2008**, *320*, 1320–1322.
- (29) Curtarolo, S.; Hart, G. L. W.; Nardelli, M. B.; Mingo, N.; Sanvito, S.; Levy, O. The High-Throughput Highway to Computational Materials Design. *Nat. Mater.* **2013**, *12*, 191–201.
- (30) Colón, Y. J.; Snurr, R. Q. High-Throughput Computational Screening of Metal-Organic Frameworks. *Chem. Soc. Rev.* **2014**, *43*, 5735–5749.
- (31) Goldsmith, J.; Wong-Foy, A. G.; Cafarella, M. J.; Siegel, D. J. Theoretical Limits of Hydrogen Storage in Metal-Organic Frameworks: Opportunities and Trade-Offs. *Chem. Mater.* **2013**, *25*, 3373–3382.
- (32) Wilmer, C. E.; Leaf, M.; Lee, C. Y.; Farha, O. K.; Hauser, B. G.; Hupp, J. T.; Snurr, R. Q. Large-Scale Screening of Hypothetical Metal-organic Frameworks. *Nat. Chem.* **2011**, *4*, 83–89.
- (33) Fernandez, M.; Woo, T. K.; Wilmer, C. E.; Snurr, R. Q. Large-Scale Quantitative Structure-Property Relationship (QSPR) Analysis of Methane Storage in Metal-Organic Frameworks. *J. Phys. Chem. C* **2013**, *117*, 7681–7689.
- (34) Chung, Y. G.; Camp, J.; Haranczyk, M.; Sikora, B. J.; Bury, W.; Krungleviciute, V.; Yildirim, T.; Farha, O. K.; Sholl, D. S.; Snurr, R. Q. Computation-Ready, Experimental Metal-Organic Frameworks: A Tool to Enable High-Throughput Screening of Nanoporous Crystals. *Chem. Mater.* **2014**, *26*, 6185–6192.
- (35) Fernandez, M.; Boyd, P. G.; Daff, T. D.; Aghaji, M. Z.; Woo, T. K. Rapid and Accurate Machine Learning Recognition of High Performing Metal Organic Frameworks for CO₂ Capture. *J. Phys. Chem. Lett.* **2014**, *5*, 3056–3060.
- (36) Kim, J.; Lin, L. C.; Martin, R. L.; Swisher, J. A.; Haranczyk, M.; Smit, B. Large-Scale Computational Screening of Zeolites for Ethane/Ethene Separation. *Langmuir* **2012**, *28*, 11914–11919.
- (37) Gee, J. A.; Zhang, K.; Bhattacharyya, S.; Bentley, J.; Rungta, M.; Abichandani, J. S.; Sholl, D. S.; Nair, S. Computational Identification and Experimental Evaluation of Metal-Organic Frameworks for Xylene Enrichment. *J. Phys. Chem. C* **2016**, *120*, 12075–12082.
- (38) Wilmer, C. E.; Farha, O. K.; Bae, Y.-S.; Hupp, J. T.; Snurr, R. Q. Structure-property Relationships of Porous Materials for Carbon Dioxide Separation and Capture. *Energy Environ. Sci.* **2012**, *5*, 9849–9856.
- (39) Lin, L. C.; Berger, A. H.; Martin, R. L.; Kim, J.; Swisher, J. A.; Jariwala, K.; Rycroft, C. H.; Bhowan, A. S.; Deem, M. W.; Haranczyk, M. In Silico Screening of Carbon-Capture Materials. *Nat. Mater.* **2012**, *11*, 633–641.
- (40) Sikora, B. J.; Wilmer, C. E.; Greenfield, M. L.; Snurr, R. Q. Thermodynamic Analysis of Xe/Kr Selectivity in over 137000 Hypothetical Metal-Organic Frameworks. *Chem. Sci.* **2012**, *3*, 2217–2223.
- (41) Van Heest, T.; Teich-mcgoldrick, S.; Greathouse, J. A.; Allendorf, M. D.; Sholl, D. S. Identification of Metal-Organic

Framework Materials for Adsorption Separation of Rare Gases: Applicability of Ideal Adsorbed Solution Theory (IAST) and Effects of Inaccessible Framework Regions. *J. Phys. Chem. C* **2012**, *116*, 13183–13195.

(42) Allen, F. H. The Cambridge Structural Database: A Quarter of a Million Crystal Structures and Rising. *Acta Crystallogr., Sect. B: Struct. Sci.* **2002**, *58*, 380–388 (accessed Sep 17, 2015)..

(43) ICSD, *Inorganic Crystal Structure Database*; Fachinformationszentrum Karlsruhe: Karlsruhe, Germany, 2006 (accessed Sep 20, 2015); <https://icsd.fiz-karlsruhe.de/search/>.

(44) Willems, T. F.; Rycroft, C. H.; Kazi, M.; Meza, J. C.; Haranczyk, M. Algorithms and Tools for High-Throughput Geometry-Based Analysis of Crystalline Porous Materials. *Microporous Mesoporous Mater.* **2012**, *149*, 134–141.

(45) Grande, C. A.; Gigola, C.; Rodrigues, A. E. Adsorption of Propane and Propylene in Pellets and Crystals of 5A Zeolite. *Ind. Eng. Chem. Res.* **2002**, *41*, 85–92.

(46) Eddaoudi, M.; Kim, J.; Rosi, N.; Vodak, D.; Wachter, J.; O’Keeffe, M.; Yaghi, O. M. Systematic Design of Pore Size and Functionality in Isoreticular MOFs and Their Application in Methane Storage. *Science* **2002**, *295*, 469–472.

(47) Park, K. S.; Ni, Z.; Côté, A. P.; Choi, J. Y.; Huang, R.; Uribe-Romo, F. J.; Chae, H. K.; O’Keeffe, M.; Yaghi, O. M. Exceptional Chemical and Thermal Stability of Zeolitic Imidazolate Frameworks. *Proc. Natl. Acad. Sci. U. S. A.* **2006**, *103*, 10186–10191.

(48) Han, S. S.; Choi, S. H.; Goddard, W. A., III. Zeolitic Imidazolate Frameworks as H₂ Adsorbents: Ab Initio Based Grand Canonical Monte Carlo Simulation. *J. Phys. Chem. C* **2010**, *114*, 12039.

(49) Coudert, F. X.; Fuchs, A. H. Computational Characterization and Prediction of Metal-Organic Framework Properties. *Coord. Chem. Rev.* **2016**, *307*, 211–236.

(50) Düren, T.; Millange, F.; Férey, G.; Walton, K. S.; Snurr, R. Q. Calculating Geometric Surface Areas as a Characterization Tool for Metal-Organic Frameworks. *J. Phys. Chem. C* **2007**, *111*, 15350–15356.

(51) Burns, R. L.; Koros, W. J. Defining the Challenges for C₃H₆/C₃H₈ Separation Using Polymeric Membranes. *J. Membr. Sci.* **2003**, *211*, 299–309.

(52) Grande, C. A.; Rodrigues, E. Propane/Propylene Separation by Pressure Swing Adsorption Using Zeolite 4A. *Ind. Eng. Chem. Res.* **2005**, *44*, 8815–8829.

(53) Gupta, A.; Chempath, S.; Sanborn, M. J.; Clark, L. a.; Snurr, R. Q. Object-Oriented Programming Paradigms for Molecular Modeling. *Mol. Simul.* **2003**, *29*, 29–46.

(54) Rappe, A. K.; Casewit, C. J.; Colwell, K. S.; Goddard, W. A., III.; Skiff, W. M. UFF, a Full Periodic Table Force Field for Molecular Mechanics and Molecular Dynamics Simulations. *J. Am. Chem. Soc.* **1992**, *114*, 10024–10035.

(55) Martin, M. G.; Siepmann, J. I. Transferable Potentials for Phase Equilibria. 1. United-Atom Description of n-Alkanes. *J. Phys. Chem. B* **1998**, *102*, 2569–2577.

(56) Wick, C. D.; Martin, M. G.; Siepmann, J. I. Transferable Potentials for Phase Equilibria. 4. United-Atom Description of Linear and Branched Alkenes and Alkylbenzenes. *J. Phys. Chem. B* **2000**, *104*, 8008–8016.

(57) Thermophysical Properties of Fluid Systems. *NIST Standard Reference Database*; National Institute of Standards and Technology: Gaithersburg, MD (accessed April 1, 2016); <http://webbook.nist.gov/>.

(58) Divekar, S.; Nanoti, A.; Daspupta, S.; Aarti; Chauhan, R.; Gupta, P.; Garg, M. O.; Singh, S. P.; Mishra, I. M. Adsorption Equilibria of Propylene and Propane on Zeolites and Prediction of Their Binary Adsorption with the Ideal Adsorbed Solution Theory. *J. Chem. Eng. Data* **2016**, *61*, 2629–2637.

(59) Böhme, U.; Barth, B.; Paula, C.; Kuhnt, A.; Schwieger, W.; Mundstock, A.; Caro, J.; Hartmann, M. Ethene/Ethane and Propene/Propane Separation via the Olefin and Paraffin Selective Metal–Organic Framework Adsorbents CPO-27 and ZIF-8. *Langmuir* **2013**, *29*, 8592–8600.

(60) Pearson, K. Mathematical Contributions to the Theory of Evolution. III. Regression, Heredity, and Panmixia. *Philos. Trans. R. Soc., A* **1896**, *187*, 253–318.

(61) Lamia, N.; Jorge, M.; Granato, M. A.; Almeida Paz, F. A.; Chevreau, H.; Rodrigues, A. E. Adsorption of Propane, Propylene and Isobutane on a Metal-Organic Framework: Molecular Simulation and Experiment. *Chem. Eng. Sci.* **2009**, *64*, 3246–3259.

(62) Bae, Y.-S.; Lee, C. Y.; Kim, K. C.; Farha, O. K.; Nickkias, P.; Hupp, J. T.; Nguyen, S. T.; Snurr, R. Q. High Propene/Propane Selectivity in Isostructural Metal-Organic Frameworks with High Densities of Open Metal Sites. *Angew. Chem., Int. Ed.* **2012**, *51*, 1857–1860.

(63) Bloch, E. D.; Queen, W. L.; Krishna, R.; Zdrozny, J. M.; Brown, C. M.; Long, J. R. Hydrocarbon Separations in Metal-Organic Framework with Open Iron(II) Coordination Sites. *Science* **2012**, *335*, 1606–1610.

(64) Kim, H.; Jung, Y. Can Metal-Organic Framework Separate 1-Butene from Butene Isomers? *J. Phys. Chem. Lett.* **2014**, *5*, 440–446.